ESC European Society of Cardiology

European Heart Journal - Cardiovascular Imaging (2018) **19**, 757–767
doi:10.1093/ehjci/jex340

Diagnostic accuracy and prognostic value of simultaneous hybrid ^{18}F-fluorodeoxyglucose positron emission tomography/magnetic resonance imaging in cardiac sarcoidosis

Eleanor C. Wicks[1,2,3]*, Leon J. Menezes[1,2,4], Anna Barnes[1,2], Saidi A. Mohiddin[1,2], Neha Sekhri[1], Joanna C. Porter[1,5], Helen L. Booth[1,5], Emily Garrett[1], Riyaz S. Patel[1,4], Menelaos Pavlou[6], Ashley M. Groves[2,4], and Perry M. Elliott[1,4]

[1]University College London Institute for Cardiovascular Science and Barts Heart Centre, St. Bartholomew's Hospital, West Smithfield, EC1A 7BE, London, UK; [2]Institute of Nuclear Medicine, University College London Hospitals, UK; [3]Oxford University Hospitals, John Radcliffe Hospital, Headley Way, Headington, Oxford, OX3 9DU, UK; [4]National Institute for Health Research University College London Hospitals and Barts Heart Biomedical Research Centres, UK; [5]Department of Respiratory Medicine, University College London Hospitals, 5th Floor, University College Hospital, 235 Euston Road, London, NW1 2BU, UK; and [6]Department of Statistical Science, University College London, London, UK

Received 2 June 2017; editorial decision 12 December 2017; accepted 15 December 2017; online publish-ahead-of-print 8 January 2018

Aims Cardiac death is the leading cause of mortality in patients with sarcoidosis, yet cardiac involvement often remains undetected. Cardiovascular magnetic resonance imaging (CMR) and ^{18}F-fluorodeoxyglucose (FDG)-positron emission tomography (PET) have been used to diagnose cardiac sarcoidosis (CS) yet never simultaneously in a cohort. This study sought to assess the diagnostic and prognostic utility of simultaneous hybrid cardiac PET/MR.

Methods and results Fifty-one consecutive patients with suspected CS (age 50 ± 13 years, 31 males) underwent simultaneous PET/MR following a high-fat/low-carbohydrate diet and 12-h fast. Blinded image analysis of FDG uptake and late gadolinium enhancement (LGE) was performed using the American Heart Association (AHA) 16-segment model. The sensitivity and specificity of PET/MR for diagnosing CS was estimated using the Japanese Ministry of Health and Welfare guidelines. The primary endpoint was a composite of death, aborted sudden cardiac death, sustained ventricular arrhythmia, complete heart block, and hospital admission with decompensated heart failure. The secondary endpoints were a fall in left ventricular ejection fraction (LVEF) >10%, non-sustained ventricular tachycardia and other cardiac-related hospital admission. The prevalence of CS was 65% ($n = 33$). The sensitivity of PET and CMR alone for detecting CS was 0.85 and 0.82, respectively. Hybrid PET/MR was superior for detecting CS with sensitivity, specificity, positive, and negative predictive values of 0.94, 0.44, 0.76, and 0.80, respectively. There was poor intermodality agreement for the location of cardiac abnormalities ($k = 0.02$). Over the median follow-up of 2.2 years, there were 18 (35%) adverse events. Cardiac RV PET abnormalities and presence of LGE were independent predictors of adverse events. Abnormalities found on both PET and magnetic resonance imaging was the strongest predictor of major adverse cardiac events.

Conclusion Simultaneous PET/MR is an accurate method for diagnosing CS. FDG-PET and CMR combined offers complementary information on disease pathophysiology. The presence of LGE and FDG uptake on PET/MR identifies patients at higher risk of adverse events. PET and CMR should therefore be considered in the assessment of disease presence, stage, and prognosis in CS.

Keywords sarcoidosis • cardiac • cardiac magnetic resonance imaging • ^{18}F-fluorodeoxyglucose • positron emission tomography • late gadolinium enhancement

*Corresponding author. Tel: +44 1865 234674. *E-mail address*: eleanor.wicks@ouh.nhs.uk

Introduction

Sarcoidosis is a multisystem inflammatory disorder characterized by non-caseating granulomata.[1–3] Clinical studies suggest that only 5% of patients with systemic sarcoidosis have overt cardiac involvement,[4] yet autopsy series report cardiac involvement in up to 50% of cases with fatal sarcoidosis,[2,5] suggesting that cardiac sarcoidosis (CS) is frequently underdiagnosed with potentially life-threatening consequences.

An endomyocardial biopsy (EMB) showing non-caseating epithelioid granulomata is the diagnostic gold standard for CS, but it has a low diagnostic yield due to the patchy distribution of disease and the frequent location of granulomatous lesions in the basal, lateral, and epicardial segments of the left ventricle wall.[6] EMB is also an invasive technique, which is not universally available or performed without risk. Consequently, the diagnosis of CS is usually made on the basis of clinical and imaging features in conjunction with biopsy evidence from an extracardiac site as proposed by the Japanese Ministry of Health and Welfare (JMHW).[7]

Late gadolinium enhancement (LGE) on cardiovascular magnetic resonance imaging (CMR) is a minor criterion in the JMHW guideline for the diagnosis of CS. LGE in this context usually represents post-inflammatory myocardial scarring[8,9] and is associated with adverse events including cardiac death.[8,10] Myocardial inflammation can be visualised using ^{18}F-fluorodeoxyglucose (FDG)-positron emission tomography (PET), but the JMHW guideline includes only gallium 67 whole body planar imaging as a non-invasive marker of disease and there are scant data comparing gadolinium-enhanced CMR and FDG-PET imaging.[11,12]

The development of hybrid positron emission tomography and magnetic resonance (PET/MR) imaging systems offers an efficient combined method for performing simultaneous structural, functional, and tissue characterization with CMR and metabolic imaging with PET. The aim of this study was to evaluate the performance of hybrid PET/MR in patients with suspected CS. We postulated that hybrid PET/MR imaging is a more accurate technique than PET or CMR when performed alone for diagnosing active cardiac involvement in sarcoidosis and that multimodality imaging improves the prediction of adverse disease-related outcomes.

Methods

Subjects and study design

The study cohort comprised consecutively evaluated patients with known or clinically suspected CS seen in our centre between April 2012 and July 2013; 7 (14%) had confirmed CS on EMB; 44 (86%) patients with suspected CS had histologically proven extracardiac sarcoidosis. Patients were classified into those with and without evidence for CS using the 2006 revised JMHW guideline (see Supplementary data online, *Table S1*).[7] The minor criterion, LGE, was excluded from this classification to enable its examination within this study.

Study exclusion criteria were: inability to give informed consent; pregnant or breast-feeding females; diabetes mellitus (due to the confounding influence of diabetes and insulin upon glucose metabolism); previous myocardial infarction or known coronary artery disease; allergy to gadolinium contrast agent; estimated glomerular filtration rate <30 mL/min/1.73 m^2); claustrophobia and the presence of an implanted device incompatible with scanning at a 3 Tesla field strength.

All subjects underwent clinical evaluation including history, physical examination, a 12-lead electrocardiogram (ECG), 2D and Doppler echocardiogram, and baseline blood tests. Patients were reviewed every 6–12 months or earlier if clinically indicated. All eligible patients provided written informed consent and the study was conducted in accordance with institutional guidelines, following IRB approval.

Patient preparation

All subjects underwent dietary preparation for 24 h prior to PET/MR scanning using a high fat content diet and avoidance of carbohydrates, sugars, dairy, or starchy foods followed by a prolonged fast for 12 h to suppress physiological myocardial FDG uptake.[13,14] Adherence was confirmed through direct questioning.

Hybrid PET/MR cardiac imaging protocol

Following dietary preparation, all patients underwent a whole body hybrid PET/MR scan using an integrated whole-body PET/MR (3.0 Tesla) scanner (Biograph mMR; Siemens Healthcare, Erlangen, Germany). All subjects received an intravenous injection of 370 MBq of FDG at a mean of 64 min (±13 min) (mean activity 157 MBq ± 39 MBq), prior to PET/MR image acquisition. PET myocardial perfusion imaging was not performed in this study to minimize radiation exposure as most subjects had already undergone coronary evaluation. A standard cardiac MR imaging protocol was performed to evaluate LGE simultaneously with FDG-PET acquisition following single breath-hold attenuation correction (see Supplementary data online, *Figure S1*).[15] T2-weighted imaging was not performed as this programme was unavailable on PET/MR at the time of this study.

Cardiac MR imaging protocol

Transverse half Fourier acquisition single-shot turbo spin-echo sequences were performed for 2D extracardiac anatomical imaging. Multiplanar balanced steady-state free precession cine sequences were acquired for wall motion abnormalities and volumetric analysis using the following acquisition parameters: voxel size 1.3 × 1.3 × 8 mm^3; repetition time of 864 ms; acquisition matrix of 123 256; echo time of 1.56 s; inversion time of 400–500 ms; flip angle of 20°; and slice thickness of 8 mm with a 2 mm gap. LGE imaging was performed using a standard segmented turbo fast low-angle shot 2D inversion-recovery gradient echo sequence 10–15 min after the bolus injection of the contrast agent injection Gadoterate meglumine, (gadolinium-DOTA, marketed as Dotarem, Guerbet S.A., Paris, France) at a dose of 0.1 mmol/kg. All images were acquired on breath hold and were ECG-triggered. The field of view was adjusted according to subject size (320–400 mm). Matching contiguous short-axis views of the entire left ventricle were obtained for cine images and LGE.

FDG PET/MR protocol

FDG images were acquired using ECG-gating and 3D image reconstruction (voxel size, 2 × 2 × 2 mm^3) using ordinary Poisson ordered-subset expectation maximization with three iterations and 21 subsets, a Gaussian filter with 5.0 mm full width at half maximum, and a 344 × 344 image matrix. For attenuation correction of the acquired PET data, a four-compartment model attenuation map was calculated using the MR capabilities of the machine using fat-only and water-only Dixon-based sequences for automatic PET attenuation correction.[16] A full stack of short axis slices was acquired of the left ventricle from base to apex to exactly match the MR slice position for direct comparison.

Image analysis

The PET and LGE images were analysed qualitatively in consensus by two experienced readers blinded to the clinical characteristics of each subject. The global myocardial appearance of FDG uptake was categorized visually into none, diffuse, and focal or focal-on-diffuse.[11,14,17–19] None and diffuse uptake were categorized as a negative scan, and focal or focal-on-diffuse was categorized as a positive scan.[11,17] Regional analysis was performed by dividing three short axis slices (base, mid, and apical) according to the conventional American Heart Association 17 segment model; 16 segments, excluding the apex, were used for analysis. Each of the 16 segments was visually assessed on a binary scale as positive for FDG tracer uptake (PET score: 1 abnormal increased uptake, 0 no increased uptake), and for the presence of LGE (LGE present 1, LGE absent 0). Quantification analysis to assess heterogeneity was calculated for PET by dividing the maximal standardized uptake value (SUV) within the myocardium by the least avid segment.[20] Co-localization of LGE with FDG uptake was evaluated using co-registered LGE-FDG images generated by fusing individually matched LGE and PET short-axis slices through 3D-image reconstruction using OsiriX shareware (Version 5.8.5, Geneva, Switzerland) (www.osirix-viewer.com). Finally, each PET/MR scan was assessed for the presence of extracardiac disease.

Clinical outcomes

Clinical information on adverse events was obtained via the electronic hospital records. The pre-specified primary end point was a composite of all-cause mortality; aborted sudden cardiac death (either ventricular tachyarrhythmia leading to appropriate cardioverter-defibrillator discharge based on stored ECGs or successfully resuscitated cardiac arrest); symptomatic sustained ventricular arrhythmia; symptomatic bradyarrhythmia leading to pacemaker implantation; or hospitalization with decompensated heart failure. The secondary endpoints were a fall in LVEF > 10%, non-sustained ventricular tachycardia, or other cardiac-related hospital admissions.

Statistical analysis

Statistical analysis was performed using SPSS (Version 23, IBM Corporation, Illinois, USA). The Kolmogorov–Smirnov analysis was performed to assess for normality. Continuous data were expressed as mean ± standard deviation (for symmetrically distributed variables) and median ± interquartile range (IQR) (for skewed variables). Categorical data were reported as frequencies and percentages. A χ^2 test was used to test the association between categorical variables, and the independent Student's *t*-test was performed to compare differences between continuous data in unrelated groups. The Bonferroni correction method was used to counteract for multiple comparisons. Segment wise (16 segments per scan) binary inter-method agreement between LGE and FDG was calculated using Cohen's kappa. The follow-up period for each patient was calculated from the date of their first evaluation at our centre to the date of the study endpoint or primary adverse event. Event-free survival and cardiac survival (time to first event) were plotted as Kaplan–Meier curves. The annual event rate according to the pattern of FDG uptake was calculated by dividing the number of patients reaching the composite endpoint by the total follow-up period for the endpoint.

Univariate Cox regression analysis was performed to explore the association between individual variables and the time to event for the composite outcome. Multivariate Cox regression analysis was performed to delineate the influence of confounding variables and the time to event, upon outcome. Overall model fit was estimated using the χ^2 analysis. To ensure suitability, the proportional hazards assumption was investigated using the Schoenfeld residuals.[21] The multivariate analysis was limited as only 18 events were observed in this relatively small cohort and a minimum of 10 cardiac events were required per coefficient estimated by the model to ensure that the regression coefficients of the model were estimated with adequate precision. This allowed for just two regression coefficients to develop the risk model and thus the findings should be interpreted with caution. Each imaging component was investigated separately and adjusted for LVEF. Hybrid PET/MR was excluded from this model due to estimation problems and perfect prediction.[22]

All statistical tests were two-tailed, 95% confidence intervals (CIs) were used to quantify certainty and a *P-value* <0.05 was considered statistically significant.

Results

A total of 51 patients [31 men and 20 women; mean age 50 ± 13 years (range 23–80); 65% Caucasian; mean LVEF 53 ± 15%], with known or clinically suspected CS were recruited. Forty-four (86%) patients had histologically proven extracardiac sarcoidosis and 7 (14%) had CS confirmed on EMB. According to the JMHW guideline, the prevalence of CS was 65% (33/51). The mean time interval between clinical suspicion of CS and PET/MR scan was 0.14 ± 0.28 years. The median follow-up time following scanning was 2.2 years (IQR 1.7–3.5 years). No patient was lost to follow-up.

Clinical characteristics of the total cohort of 51 patients and JMHW± sub-groups are described in *Table 1*. There was no significant difference between groups in age, sex, self-reported ethnicity, incidence of coronary risk factors, immunosuppression use, or NYHA functional class. However, LVEF was lower in the JMHW+ subgroup (48% vs. 62%; $P = 0.001$, 95% CI 5.8–21.6).

Imaging findings

Twenty-eight (55%) patients showed abnormal cardiac PET findings (17 focal and 11 focal on diffuse uptake); twenty-three (45%) patients had negative cardiac PET findings [19 no cardiac uptake (i.e. complete suppression of FDG uptake) and four with a diffuse pattern] (*Table 2*). Four patients had abnormal PET findings in the right ventricle. One patient who had diffuse uptake had histological confirmation of active CS on EMB. Within the JMHW+ subgroup, PET abnormalities were more frequent when compared with their JMHW- counterparts although this did not reach statistical significance (61% vs. 44%; $P = 0.27$). PET quantification analysis also confirmed that those fulfilling the JMHW criteria had greater SUV heterogeneity between different segments of the myocardium (when measured using the SUVmax to least avid segment ratio) than those JMHW- (mean 1.94 ± 1.69 vs. 1.29 ± 0.38; $P = 0.04$). Extracardiac abnormalities (in the form of lymphadenopathy or lymph node avidity, parenchymal disease or multi-system involvement with sarcoidosis) were seen in 29 (57%) of subjects.

LGE was present in 32 (63%) patients and was more frequent in the JMHW+ subgroup (82% vs. 22%; $P < 0.01$). When PET and LGE abnormalities were considered together, 8 (16%) patients had no abnormalities, 11 (22%) subjects had PET abnormalities only, 15 (29%) subjects had LGE only, and 17 (33%) had both PET and CMR abnormalities. PET/MR abnormalities were more frequently seen within the JMHW+ group compared with the JMHW- group (49% vs. 6%; $P = 0.005$).

The regional distribution of FDG-PET uptake and LGE in patients with CS according to JMHW guideline is presented in *Figure 1*. There

Table 1 Clinical characteristics of all study population ($n = 51$) and by subgroup

Characteristics	Total cohort ($n = 51$)	CS by JMHW + ($n = 33$)	CS by JMHW − ($n = 18$)	Patients with adverse events ($n = 18$)	Patients without adverse events ($n = 33$)
Age (years)	50.1 ± 13	51.8 ± 13	46.8 ± 12	50.0 ± 12	50.1 ± 13
Age at diagnosis (years)	43 ± 13	44 ± 13	40 ± 13	43 ± 12	42 ± 14
Male sex (%)	31 (61)	21 (64)	10 (56)	14 (78)	11 (33)
Caucasian (%)	33 (65)	24 (73)	9 (50)	14 (78)	19 (58)
Afro-Caribbean (%)	8 (16)	4 (12)	4 (22)	0 (0)	8 (24)
Symptoms (%)					
Chest pain	19 (37)	10 (30)	9 (50)	4 (22)	15 (46)
Dyspnoea	27 (53)	19 (58)	8 (44)	11 (61)	16 (49)
Palpitations	24 (47)	19 (58)	5 (28)	15 (83)	9 (27)
Syncope	10 (20)	6 (18)	4 (22)	4 (22)	6 (18)
Presyncope	11 (22)	9 (27)	2 (11)	6 (33)	5 (15)
Hypertension (%)	7 (14)	5 (15)	2 (11)	5 (28)	2 (6)
Hypercholesterolaemia (%)	9 (18)	7 (21)	2 (11)	4 (22)	5 (15)
Family history sarcoidosis (%)	6 (12)	1 (2)	2 (11)	0 (0)	3 (9)
Histologically confirmed (%)					
Cardiac (EMB) sarcoidosis	7 (14)	7 (21)	0 (0)	5 (28)	2 (6)
Extracardiac sarcoidosis	44 (86)	25 (76)	14 (78)	14 (78)	25 (76)
NYHA (%)					
I	31 (61)	20 (61)	11 (61)	1 (55)	21 (64)
II	17 (33)	10 (30)	7 (39)	5 (28)	12 (36)
III	3 (6)	3 (9)	0 (0)	3 (17)	0 (0)
IV	0 (0)	0 (0)	0 (0)	0 (0)	0 (0)
LV ejection fraction (%)	53 ± 15	48 ± 16	62 ± 6	44 ± 14	58 ± 13
Clinical phenotype recorded at baseline (%)					
LVH	13 (25)	8 (24)	5 (28)	3 (17)	10 (30)
DCM	18 (35)	19 (58)	1 (6)	12 (67)	8 (24)
LVEF <50%	23 (45)	23 (70)	0 (0)	13 (72)	10 (30)
Decompensated heart failure	6 (12)	6 (18)	0 (0)	5 (28)	1 (3)
Conduction disease	6 (12)	19 (42)	2 (11)	6 (33)	10 (30)
CHB	2 (4)	1 (3)	0 (0)	1 (3)	0 (0)
Ventricular arrhythmia	8 (16)	7 (21)	1 (6)	5 (28)	3 (9)
Acute presentation	10 (20)	9 (27)	2 (11)	8 (44)	3 (9)
Serum ACE level (mg/mL)	35 ± 39	25 ± 30	52 ± 48	29 ± 32	38 ± 43
NT pro BNP (μg/mL)	52 ± 95	69 ± 112	20 ± 32	92 ± 112	30 ± 77
Immunosuppression at the time of scan	19 (37)	14 (42)	7 (39)	8 (44)	13 (39)
Corticosteroids	16				
Methotrexate	3				
Hydroxychloroquine	4				
Azathiaprine	2				
Mycophenalate mofetil	2				
Cyclophosphamide	1				
Abnormal ECG	35	32 (97)	7 (39)	18 (100)	21 (64)
Basal thinning	21 (41)	19 (58)	3 (17)	10 (56)	12 (36)
Device therapy at study end	13 (25)	10 (32)	3 (17)	6 (33)	7 (21)
Pacemaker	2 (4)	1 (3)	1 (6)	0 (0)	2 (6)
ICD	8 (16)	7 (21)	1 (6)	6 (33)	2 (6)
CRTD	1 (2)	1 (3)	0 (0)	0 (0)	1 (3)
ILR	2 (4)	1 (3)	1 (6)	0 (0)	2 (6)

Values are represented as *n* (%) or mean ± SD unless otherwise stated.

Hypertension is defined as a blood pressure persistently measuring greater than 140/90. Hypercholesterolaemia is defined as a total cholesterol measuring >5 mmol/L and LDL <3 mmol/L. LVH is defined by a maximal LV wall thickness >13 mm. Dilated cardiomyopathy is defined by an LVEDD (% predicted) >112% and LVFS < 25%. The clinical phenotype describes the clinical characteristics noted at baseline. Immunosuppression was noted at the time of PET/MR scanning. Device therapy was noted at study end. ECG abnormalities were defined according to the JMHW criteria.

ACE, angiotensin converting enzyme; BNP, brain natriuretic peptide; CHB, complete heart block; CRTD, cardiac resychronization therapy with defibrillator; CS, cardiac sarcoidosis; DCM, dilated cardiomyopathy; ECG, electrocardiogram; EMB, endomyocardial biopsy; ICD, implanted cardiovertor defibrillator; ILR, implantable loop recorder; JMHF, Japanese Ministry of Health and Welfare; LV, left ventricle; LDL, low density lipoprotein; LVEDD, left ventricular end-diastolic diameter; LVEF, left ventricle ejection fraction on echocardiography; LVFS, left ventricle fractional shortening; LVH, left ventricular hypertrophy; NYHA, New York Heart Association; PET/MR, positron emission tomography/magnetic resonance imaging; SD, standard deviation.

Table 2 Comparison of imaging abnormalities within the whole study population and according to subgroup categorization (JMHW criteria and by occurrence of an adverse event)

Characteristics	Total cohort ($n = 51$)	CS by JMHW + ($n = 33$)	CS by JMHW − ($n = 18$)	*P*-value	Patients with adverse events ($n = 18$)	Patients without adverse events ($n = 33$)	*P*-value
Presence of LGE (%)	32 (63)	27 (82)	4 (22)	<0.05	17 (94)	14 (42)	<0.01
Cardiac PET findings (%)	28 (55)	20 (61)	8 (44)	0.27	13 (72)	15 (46)	0.06
No abnormalities	19 (37)	11 (14)	8 (44)		3 (17)	16 (49)	
Focal	17 (33)	14 (42)	1 (6)		10 (56)	7 (21)	
Focal on diffuse	11 (22)	6 (18)	5 (28)		3 (17)	8 (24)	
Diffuse	4 (8)	2 (6)	2 (11)		2 (11)	2 (6)	
RV FDG uptake	4 (8)	2 (3)	2 (11)	0.61	2 (11)	2 (3)	0.61
SUVmax: least avid ratio	1.71 ± 1.41	1.94 ± 1.69	1.29 ± 0.38	0.04	2.42 ± 2.15	1.33 ± 0.43	0.001
Extracardiac sarcoidosis on PET (%)	29 (57)	17 (52)	12 (67)	0.30	6 (33)	23 (70)	0.01
Extra-cardiac ± cardiac PET abnormality (%)	36 (71)	28 (85)	8 (44)	<0.005	14 (78)	24 (73)	0.70
Hybrid PET/MR				<0.05			<0.05
PET-/MR-	8 (16)	3 (9)	5 (28)		0 (0)	8 (24)	
PET+/MR-	11 (22)	14 (42)	7 (39)		1 (9)	10 (30)	
PET-/MR+	15 (29)	10 (30)	5 (28)		5 (33)	10 (30)	
PET+/MR+	17 (33)	16 (49)	1 (6)		12 (71)	5 (15)	

Data is reported as frequencies and % or mean ± SD unless otherwise stated.
FDG, fluorodeoxyglucose; JMHW, Japanese Ministry of Health and Welfare Guidelines; LGE, late gadolinium enhancement; PET/MR, positron emission tomography/magnetic resonance imaging; RV, right ventricle; SUVmax, maximal standardized uptake value; +, presence of an abnormality on either imaging technique; -, absence of an imaging abnormality.

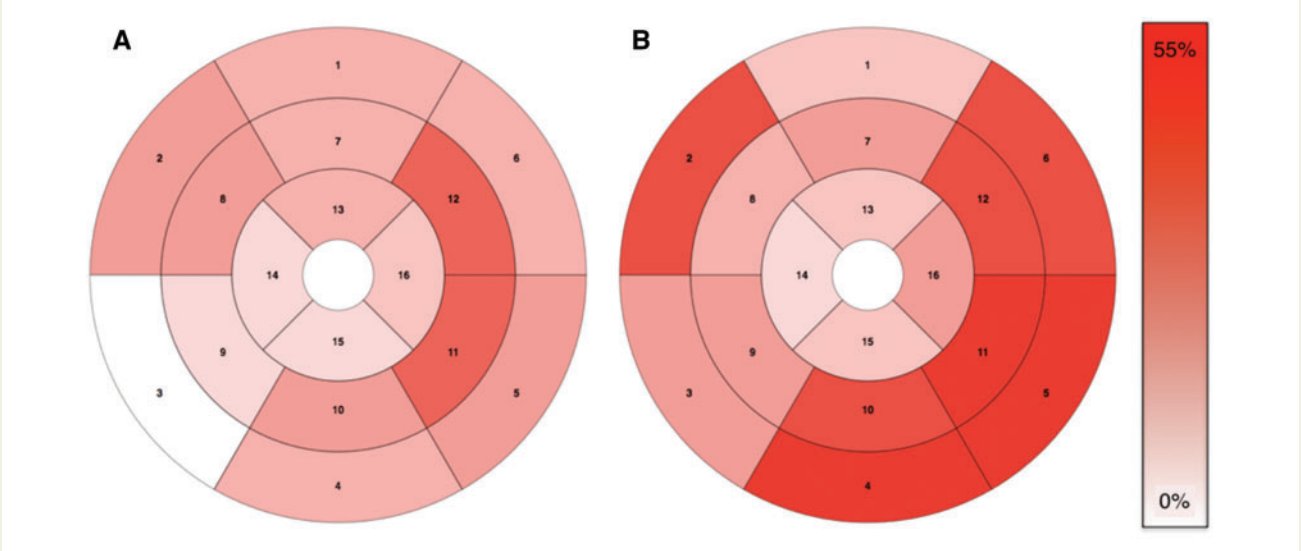

Figure 1 Regional distribution of FDG-PET uptake (*A*) and of LGE (*B*) in JMHW positive cardiac sarcoidosis group ($n = 33$) according to the AHA 16 segment model. The colour scale demonstrates an increasing proportion of segments (from 0% to 55%) with abnormal PET uptake (*A*) or the presence of LGE (*B*). This figure highlights the basal anteroseptum and inferolateral predominance of FDG uptake and LGE. AHA, American Heart Association; JMHW, Japanese Ministry of Health and Welfare; LGE, late gadolinium enhancement; PET, positron emission tomography.

was a preponderance of FDG-PET uptake and LGE in the basal to mid septum and inferolateral segments. FDG-PET uptake was more extensive than LGE [277 (34%) vs. 163 (20%) segments; kappa 0.14 (SE 0.02; 95% CI 0.10–0.18)]. There was poor inter-method agreement for the regional distribution of FDG uptake and LGE [kappa 0.021 (SE 0.041; 95% CI -0.059 to 0.101)]. Examples of patients with concordant and discordant FDG uptake and LGE are illustrated in *Figures 2 and 3*.

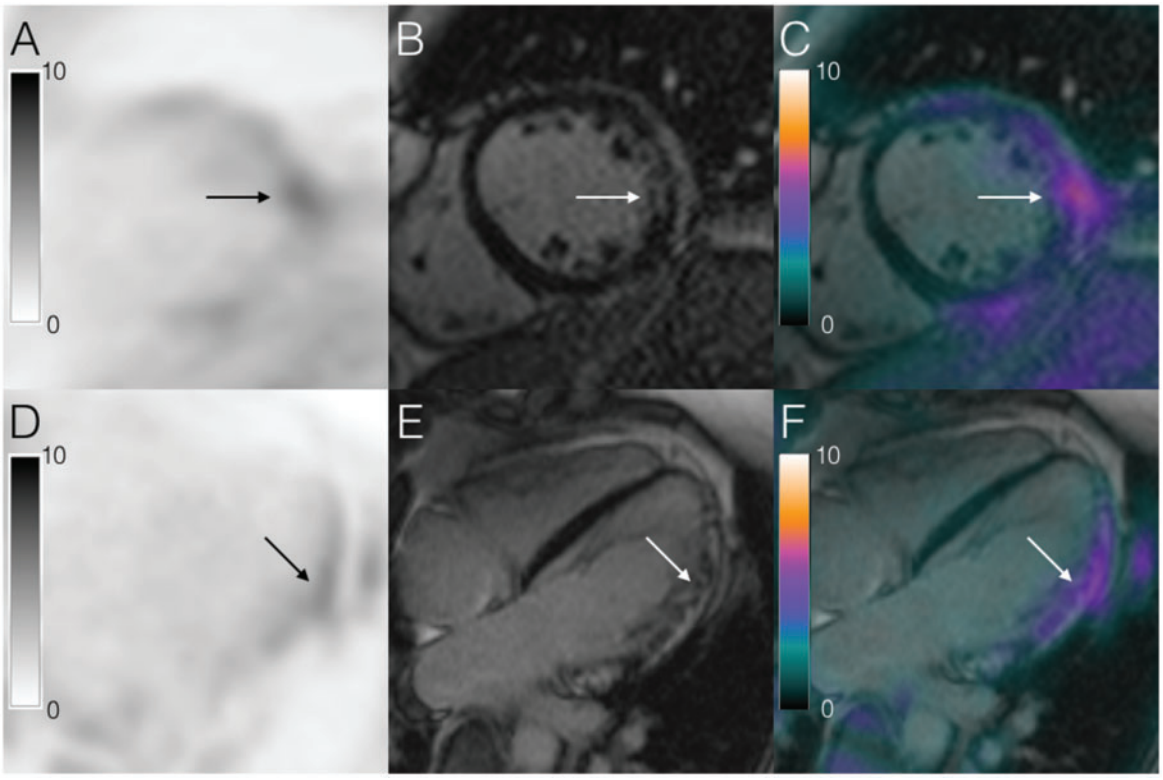

Figure 2 Hybrid imaging example of concordant LGE vs. FDG uptake PET-MR images in a patient with biopsy-proven cardiac sarcoidosis. (*A–F*) Illustrate short and long axis imaging demonstrating a concordant pattern of overlying inflammation and LGE (fibrosis). (*A* and *D*) MIP images depicting lateral FDG uptake (arrow) are shown. (*B* and *E*) Demonstrate patchy epicardial and mid-myocardial LGE (arrow), which when fused (*C* and *F*) demonstrate overlying LGE and FDG uptake (arrow highlighting the area of abnormality). FDG, fluorodeoxyglucose; LGE, late gadolinium enhancement; MIP, maximum intensity projection; PET, positron emission tomography.

The diagnostic performance of PET and LGE was also analysed (*Table 3*). Using the JMHW criteria as the gold standard, the sensitivity, and specificity for diagnosing CS with myocardial FDG PET alone were 60% and 56% (PPV 71%, NPV 44%) (AUC 0.58), respectively. When extracardiac abnormalities were considered together with abnormal myocardial uptake, the diagnostic sensitivity and specificity for PET rose to 85% and 56%, respectively (PPV 78%, NPV 67%; AUC 0.7). For LGE, the sensitivity and specificity for diagnosing CS were 82% and 78% (PPV 87%; NPV 79%; AUC 0.8). For hybrid PET/MR, the sensitivity was 94%; specificity 44%; PPV 76%; NPV 80%; AUC 0.7.

Patient outcomes

Over a median follow-up duration of 2.2 years, 18 patients (35%) had adverse cardiac events, 16 of which were primary end-points, and two secondary end-points. One (2%) patient died from acute AV block, 10 (20%) had symptomatic sustained ventricular tachyarrhythmia leading to appropriate defibrillator discharge, 5 (10%) were hospitalized for decompensated heart failure and 2 (4%) were admitted to hospital for other cardiac-related events (atrial arrhythmias necessitating ablation). No other patients developed atrioventricular block requiring pacemaker implantation during the course of the study.

Those who suffered a cardiac event were more likely to have a lower LVEF and to meet the JMHW criteria than those without a cardiac event (LVEF 44% vs. 57%, $P < 0.001$; JMHW 89% vs. 52%; $P = 0.007$).

Clinical outcomes according to the PET/MR scan findings are illustrated using Kaplan–Meier survival curves (*Figure 4*). In the eight patients with normal scan findings, there were no adverse events. In the 11 patients with abnormalities on PET imaging only (PET + LGE-), there was one event (9%). In the 15 patients with LGE on PET/MR but no FDG uptake (LGE + PET-), there were five events (33%). In the 17 individuals with abnormal PET and LGE imaging (PET + LGE+), there were 12 events (71%) (*Table 2*, *Figure 4A*). Abnormalities detected on both PET and CMR was the strongest predictor of major adverse cardiac events when compared with the absence or singular abnormalities in either PET or LGE ($P = 0.009$) (*Figure 4A*) even after adjusting for age, sex, and LVEF (*Figure 4B*).

The annualised event rates for patients with 'focal', 'focal on diffuse', 'complete suppression' of cardiac uptake, and 'diffuse uptake' were 28%, 13%, 8%, and 24%, respectively ($P = 0.26$). Patients with diffuse FDG uptake had a higher event rate than those with complete suppression of myocardial FDG uptake (24% vs. 8%; $P < 0.05$). Patients with greater myocardial heterogeneity also had a higher event rate (SUVmax: least avid ratio 2.42 ± 2.2 vs. 1.33 ± 0.4;

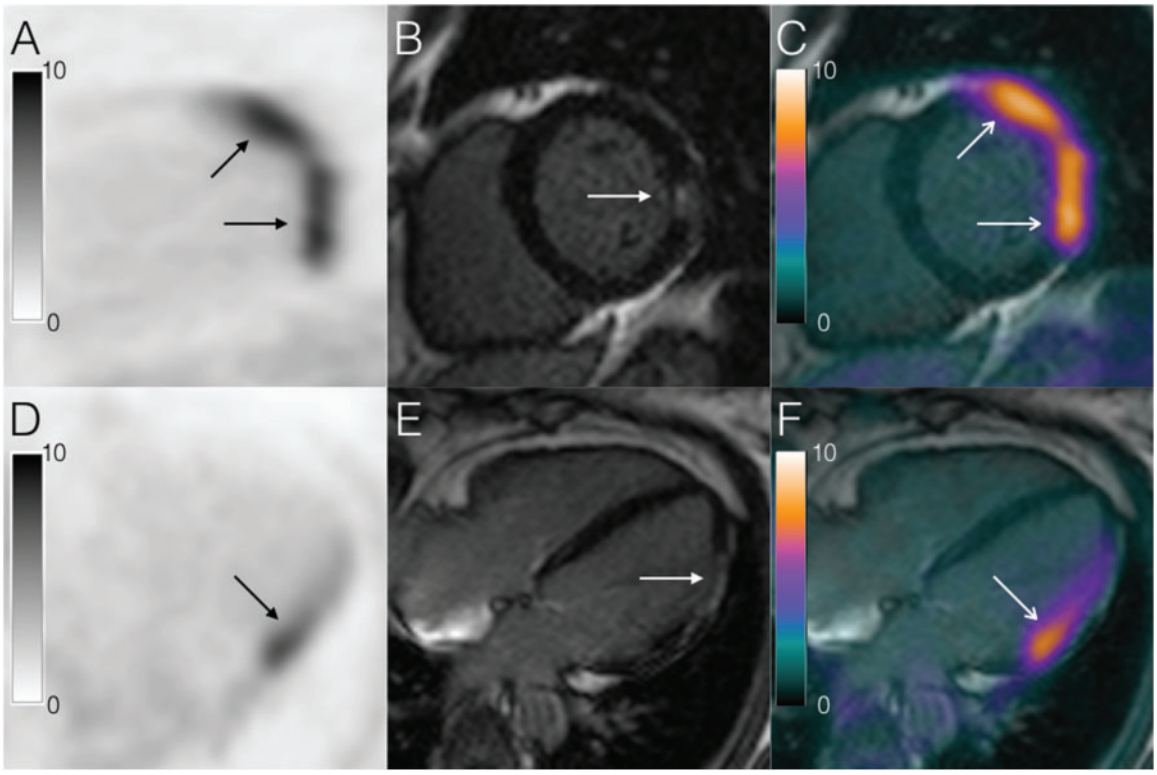

Figure 3 Hybrid imaging example of discrete, independent, discordant regions of FDG uptake (regions of inflammation), and LGE (scar) in a patient with biopsy-proven cardiac sarcoidosis. (*A–F*) Illustrate short and long axis imaging demonstrating a discordant pattern of FDG uptake (acute inflammation) surrounding the presence of LGE (scar). (*A* and *D*) MIP images depicting lateral FDG uptake are shown. (*B* and *E*) Demonstrate patchy epicardial and mid-myocardial LGE, which when fused (*C* and *F*) demonstrate discordant LGE and FDG uptake (the arrows highlight the area of abnormality). FDG, fluorodeoxyglucose; LGE, late gadolinium enhancement; MIP, maximum intensity projection; PET, positron emission tomography.

Table 3 The diagnostic performance of PET and LGE in cardiac sarcoidosis

	Sensitivity	Specificity	PPV	NPV	OR	AUC
Cardiac PET abnormality	60 (0.42–0.77)	56 (0.30–0.78)	71 (0.51–0.87)	44 (0.23–0.66)	1.92 (0.60–6.20)	0.58
Extra-cardiac ± cardiac PET abnormality	85 (0.68–0.95)	56 (0.31–0.78)	78 (0.61–0.90)	67 (0.38–0.88)	7 (1.85–26.5)	0.70
LGE on MRI	82 (0.65–0.93)	78 (0.52–0.94)	87 (0.70–0.96)	79 (0.46–0.88)	15.8 (3.80–65.2)	0.80
Hybrid PET/MR	94 (0.80–0.99)	44 (0.22–0.69)	76 (0.60–0.88)	80 (0.44–0.97)	12.4 (2.25–68.3)	0.70

Sensitivity, specificity, and diagnostic odds ratio to evaluate the effectiveness of FDG-PET and LGE when performed alone vs. utilising hybrid PET/MR when regressed against the JMHW guidelines as the reference standard (confidence interval).
AUC, area under the curve; JMHW, Japanese Ministry of Health and Welfare Guidelines; LGE, late gadolinium enhancement; NPV, negative predictive value; OR, diagnostic odds ratio; PET/MR, positron emission tomography/magnetic resonance imaging; PPV, positive predictive value.

$P = 0.001$). There was no association between the presence of extra-cardiac FDG uptake or number of affected systemic organs and adverse events.

For LGE, the annualised event rate in the presence of LGE was 25% vs. 3% when LGE was absent. One of the 19 subjects (5%) without LGE had a hospital admission for atrial fibrillation ($P < 0.05$).

Univariate predictors of adverse events are described in *Table 4*. PET and LGE imaging components were considered separately within multivariate analyses. Hybrid PET/MR was excluded because of estimation problems due to absence of events in the PET/MR negative group (perfect prediction). Cardiac PET abnormalities when analysed independently were not predictive of primary adverse events [hazard ratio (HR) 2.29, 95% CI 0.72–7.32; $P = 0.16$)] although RV avidity was predictive of adverse outcomes after adjusting for LVEF (HR 5.84, 95% CI 1.12–30.4; $P < 0.04$) (*Table 5*). The presence of LGE was an independent predictor of major adverse cardiac events after adjusting

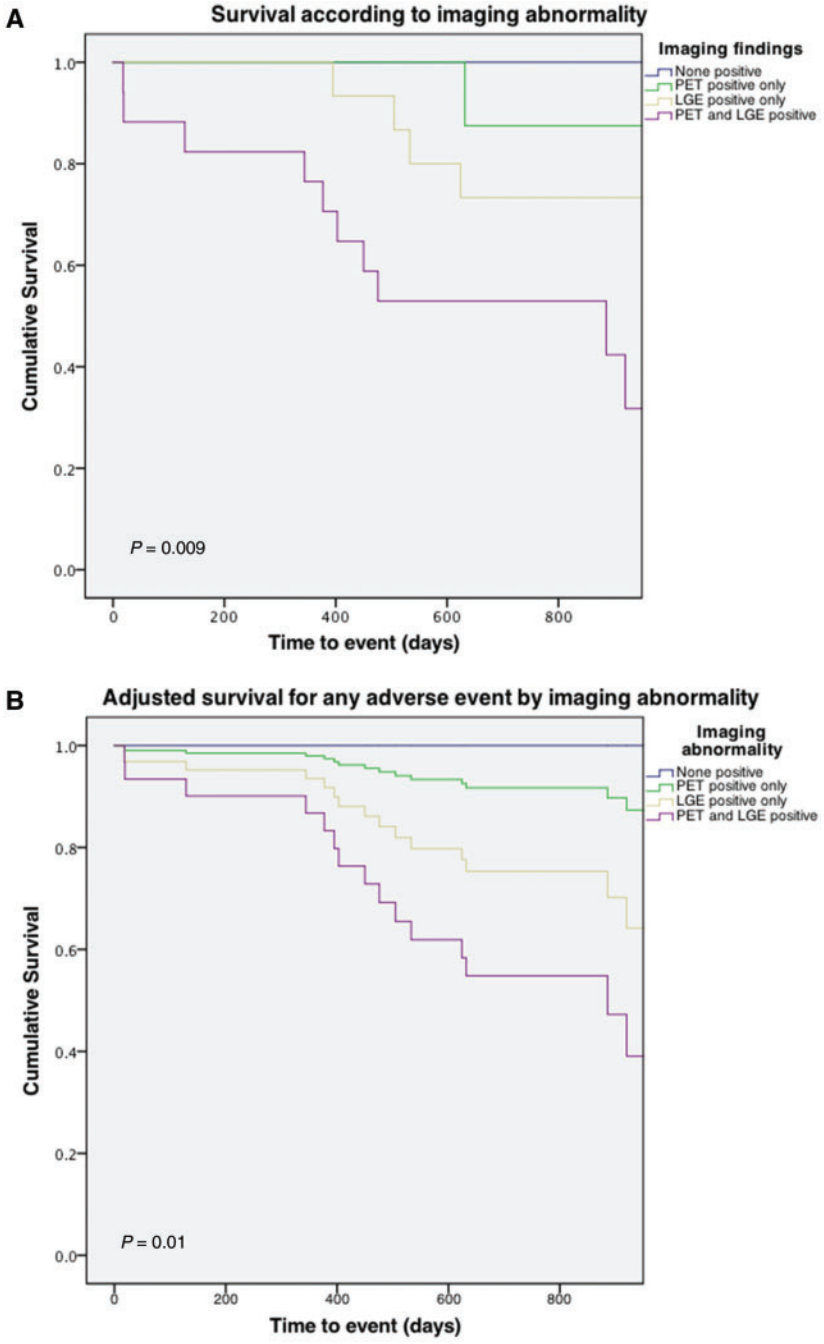

Figure 4 The Kaplan–Meier survival curves for all pre-specified end points. (*A*) Using the log-rank statistical method, this graph demonstrates a worse survival as the number of abnormalities detected on PET or cardiac MRI imaging increases. (*B*) Demonstrates the adjusted survival analysis for imaging abnormalities and adverse event having adjusted for age, sex, and LVEF using the multivariate Cox regression analysis (χ^2 value 16.8, $P = 0.01$). It illustrates an adverse prognosis as subjects progress from PET positivity only, to LGE positivity and both PET/MR positivity. LVEF, left ventricle ejection fraction; LGE, late gadolinium enhancement; PET, positron emission tomography.

for LVEF on multivariate analysis (HR 8.04, 95% CI 1.02–63.8; $P = 0.02$) (*Table 6*, *Figure 4B*). This adverse effect persisted after adjusting for age, sex, LVEF, and cardiac abnormalities found on PET (*Table 7*, *Figure 4B*).

In patients with CS according to the JMHW guidelines, the event rate and cardiac death rate was significantly higher than their JMHW-negative counterparts at 49% and 3% (vs. 11% and 0%, respectively; $P = 0.008$). Fulfillment of the JMHW criteria was associated with an increased risk of an adverse event (HR 9.4, CI 1.24–71.7; $P < 0.05$). Given the small study population and the small number of events, further statistical comparison between survival curves was not performed.

Table 4 Univariate Cox proportional hazards regression analysis of primary vs. any adverse events

Predictor	Primary event			Any event		
	Model fit χ^2 (*P*-value)	Hazard ratio (95% CI)	*P*-value	Model fit χ^2 (*P*-value)	Hazard ratio (95% CI)	*P*-value
Univariate variables						
Age (years)	0.34 (0.55)	0.99 (0.95–1.03)	0.51	0.04 (0.84)	1.0 (0.96–1.03)	0.84
Male sex	2.21 (0.14)	2.10 (0.77–5.71)	0.15	2.07 (0.15)	1.98 (0.77–5.09)	0.57
Initial LVEF %	5.78 (0.02)	0.97 (0.94–0.99)	0.02	5.61 (0.02)	0.97 (0.94–1.0)	0.02
History of VT	13.0 (<0.001)	5.67 (1.98–16.2)	0.001	13.2 (<0.001)	5.27 (1.96–14.1)	0.001
JMHW criteria +	7.01 (0.008)	9.44 (1.24–71.7)	0.03	5.70 (0.02)	5.04 (1.15–22.0)	0.03
Cardiac PET+ findings (%)	2.06 (0.15)	2.29 (0.72–7.32)	0.16	1.67 (0.20)	1.99 (0.69–5.74)	0.20
RV FDG uptake	1.85 (0.17)	2.75 (0.6–12.57)	0.19	1.56 (0.21)	2.53 (0.56–11.42)	0.23
Extracardiac sarcoidosis on PET (%)	4.39 (0.04)	0.34 (0.11–0.98)	0.05	6.70 (0.01)	0.28 (0.10–0.78)	0.02
Extra-cardiac + cardiac PET abnormality (%)	0.17 (0.68)	1.31 (0.36–4.69)	0.68	0.004 (0.95)	1.04 (0.33–3.22)	0.95
Presence of LGE (%)	8.10 (0.004)	10.63 (1.4–80.78)	0.02	9.11 (0.003)	11.7 (1.55–88.1)	0.02
RV LGE	21.2 (<0.001)	9.22 (2.94–28.94)	<0.001	19.1 (<0.001)	8.0 (2.65–24.1)	<0.001

Overall model fit estimated using χ^2 (*P*-value). Hybrid PET/MR has been excluded due to perfect prediction and the small sample size.
CI, confidence interval; FDG, fluorodeoxyglucose; JMHW, Japanese Ministry of Health and Welfare Guidelines; LVEF, left ventricle ejection fraction measured by echocardiography; LGE, late gadolinium enhancement; PET/MR, positron emission tomography/magnetic resonance imaging; PET+, presence of an abnormality on PET; RV, right ventricle; VT, ventricular tachycardia.

Table 5 Multivariate analysis for a primary adverse event for PET after adjusting for LVEF

Predictor	Hazard ratio (95% CI)	*P*-value
Overall model fit estimated using χ^2 (7.07), $P \leq 0.03$		
Initial LVEF %	0.97 (0.94–1.00)	0.03
Cardiac PET+ findings	2.07 (0.64–6.72)	0.23
Overall model fit estimated using χ^2 (8.72), $P = 0.01$		
Initial LVEF %	0.96 (0.93–0.99)	0.007
Cardiac RV PET+ findings	5.84 (1.12–30.4)	0.036

Hybrid PET/MR has been excluded due to perfect prediction and the small sample size.
CI, confidence interval; LVEF, left ventricle ejection fraction measured by echocardiography; PET/MR, positron emission tomography/magnetic resonance imaging; PET+, presence of an abnormality on PET; RV, right ventricle.

Table 6 Multivariate analysis for a primary adverse event for LGE after adjusting for LVEF

Predictor	Hazard ratio (95% CI)	*P*-value
Overall model fit estimated using χ^2 (12.1), $P = 0.002$		
Initial LVEF %	0.98 (0.95–1.01)	0.18
Presence of LGE	8.04 (1.02–63.8)	0.02
Overall model fit estimated using χ^2 (24.6), $P < 0.001$		
Initial LVEF %	0.94 (0.91–0.98)	0.001
Presence of RV LGE	25.0 (6.00–104.1)	<0.001

Hybrid PET/MR has been excluded due to perfect prediction and the small sample size.
CI, confidence interval; LVEF, left ventricle ejection fraction measured by echocardiography; LGE, late gadolinium enhancement; PET/MR, positron emission tomography/magnetic resonance imaging; RV, right ventricle.

Discussion

This study is the first to describe the use of simultaneous PET/MR imaging in the diagnosis of CS. We have shown that this approach improves diagnostic sensitivity and the ability to risk-stratify patients according to the presence of scar and inflammation. The lower specificity of hybrid PET/MR compared to performing PET or LGE on CMR alone likely reflects the capability of the technique to detect pre-clinical stages of disease that are not included in the JMHW criteria which were used as the gold standard in this study. The relatively poor correlation between PET and LGE with respect to localization of myocardial abnormalities reflects the different stages of disease at the time of imaging and suggests that the two modalities provide complementary information on disease pathophysiology.

CS can precede, follow or be concurrent with involvement of other organs. The most common presentations of CS are atrioventricular nodal block, ventricular tachycardia, and atrial arrhythmia, but extensive infiltration may also present with congestive cardiac failure and dilated cardiomyopathy. Because of its potential to cause life-threatening arrhythmias and heart failure, early diagnosis of CS is essential.

CMR provides a rapid, high-resolution, non-invasive method for diagnosing subclinical, or clinically manifest CS. In the acute phase, CMR can show myocardial oedema and LV wall thickening, but CS is more frequently characterized by areas of left ventricular wall thinning and delayed gadolinium enhancement. The myocardial enhancement in both active inflammatory and advanced stages of CS shows various patterns including a mid-myocardial and sub-epicardial LGE

Table 7 Multivariate analysis for any adverse event

Predictor	Hazard ratio (95% CI)	*P*-value
Initial LVEF %	0.98 (0.95–1.02)	0.29
Age (years)	1.02 (0.98–1.06)	0.37
Sex	1.62 (0.58–4.52)	0.35
Cardiac PET+ findings (%)	1.94 (0.61–6.16)	0.26
Presence of LGE (%)	8.75 (1.07–71.26)	0.04

Overall model fit estimated using χ^2 15.8, $P = 0.008$. Hybrid PET/MR has been excluded due to perfect prediction and the small sample size.
CI, confidence interval; LGE, late gadolinium enhancement; LVEF, left ventricle ejection fraction measured by echocardiography; PET+, presence of an abnormality on PET.

pattern and in a study of 58 patients with biopsy-proven pulmonary sarcoidosis, CMR had a 100% sensitivity for CS when using the JMHW criteria as the gold standard.[23] However, its specificity was only 78% and positive predictive value 55%, partly reflecting the non-specific nature of some patterns of LGE. Two recent meta-analyses examining 694 and 760 patients, respectively, have shown that LGE is associated with an adverse risk in patients with suspected or known CS.[24,25]

Several radionuclide techniques have been used to image systemic sarcoidosis but compared to FDG-PET, most have low sensitivity and limited spatial resolution for the detection of extra-pulmonary disease. Active inflammatory cells have high glycolytic activity and as a result have an 8-fold increase in ATP production than at baseline.[26] After crossing the cellular membrane via glucose transporters, FDG and glucose are phosphorylated by hexokinase, but FDG remains trapped within the cells and so can be imaged with PET. Unlike CMR, which detects areas of interstitial expansion caused by oedema or fibrosis, FDG PET detects active inflammatory cellular infiltrates. Several studies have suggested that FDG PET has a higher sensitivity and better spatial resolution for CS than single photon emitters such as technetium-99m, thallium-201 or gallium[17,18,19,27,28] although the specificity often remains low. A meta-analysis of FDG PET,[20] including seven studies and 164 patients, calculated a pooled sensitivity of 89% and specificity of 78% for detecting CS.

The interpretation of FDG PET for CS is complex but predominantly visual.[13,17,27–29] Semi-quantitative methods have shown that heterogeneity of PET uptake (measured by coefficient of variance or ratios of SUV uptake) may be more discriminatory.[30] The observation that patients with diffuse uptake (classified traditionally as a normal scan) have more events in this study, suggests that active disease may be missed on visual interpretation and that diffuse myocardial uptake may indeed be representative of myocardial disease in some patients.

There are few data comparing FDG-PET and CMR in cardiovascular imaging[31–34] and even fewer in patients with suspected CS.[30,35] There is no series using contemporaneous scans, an important consideration as imaging findings can change with disease evolution and treatment. This study suggests that CMR and PET demonstrate different facets of the disease which together better describe the activity and extent of disease. Gadolinium-enhanced CMR identifies expansion of the extracellular space, which is most prominent when fibrosis is present and thus may be better seen in later stages of disease. In contrast, areas of active inflammatory cellular infiltration with little oedema may be better detected using FDG.[31,32,36,37] A recent study of hybrid simultaneous PET/MR in myocarditis demonstrated good spatial agreement between LGE and FDG uptake and agreement between PET and oedema sensitive T2 weighted imaging.[32,34] PET/MR therefore offers enormous potential in the assessment of CS.

Study limitations

Although several studies have attempted to determine the accuracy of cardiac PET for diagnosing CS, all (including this study) have used the JMHW criteria as the reference standard. This may have an influence on the calculated sensitivity and specificity for CS in this study as the JMHW criteria have not been validated against any other standard and omit reference to PET for the diagnosis of CS. The Heart Rhythm Society have recently proposed new guidelines for the diagnosis of CS which may improve diagnostic accuracy but require prospective evaluation.[38]

Image acquisition, interpretation, and classification using PET is based upon internationally agreed methods. The European Association of Nuclear Medicine (EANM) Research Initiative (EARL) accreditation programme for standardization of PET acquisition and reconstruction to enable independent quality control and assurance of PET, is only available for PETCT but not yet for PETMR and therefore was not used in this study.[39] Whilst image interpretation is internationally defined, further understanding of normal fasting myocardial uptake patterns using FDG in controls is required. It is also possible that other novel tracers, such as the macrophage-directed somatostatin receptor ligands (^{68}Galium DOTA-TOC or ^{68}Gallium DOTA-TATE), may provide some advantages over FDG.[40,41] CS is also associated with resting perfusion defects, however we did not perform PET perfusion evaluation as this would have incurred an additional radiation dose. Moreover, the local protocol for CMR did not include perfusion assessment as routine and as most patients had previously undergone coronary angiography this was excluded from the protocol. Similarly, the imaging protocol did not include T2-weighted imaging as this technique was not available for PET/MR at the time of study. T2-weighted imaging techniques may offer improved sensitivity for identifying myocardial oedema in the acute phases of CS.[42,43] The use of 3D whole heart imaging datasets may also improve specificity and minimise image misregistration. Finally, among patients who are already on immunosuppressive medications, both CMR and PET may have reduced sensitivity to detect CS.[30] In our study, 37% of the cohort was taking immunosuppressive therapy at the time of scanning.

Conclusion

The presence of LGE and FDG uptake on hybrid cardiac PET/MR identifies patients at higher risk of death, arrhythmia, and decompensated heart failure and should be considered in the assessment of all patients presenting with suspected CS to determine disease activity and prognosis. Further studies are required to evaluate the potential of these imaging modalities for guiding and monitoring treatment.

Supplementary data

Supplementary data are available at *European Journal of Echocardiography* online.

Acknowledgements

We express our gratitude to the staff and patients of UCLH, The Heart Hospital and at Barts Heart Centre for their support with this study.

Funding

This study was part funded and supported by the National Institute for Health Research University College London Hospitals and Barts Heart Centre Biomedical Research Centres. St. Bartholomew's Hospital is also a member of the European Reference Network on Rare and Complex Diseases of the Heart (Guard-Heart; http://guard-heart.ern-net.eu).

Conflict of interest: None declared.

References

1. Roberts WC, McAllister HA Jr, Ferrans VJ. Sarcoidosis of the heart. A clinicopathologic study of 35 necropsy patients and review of 78 previously described necropsy patients. *Am J Med* 1977;**63**:86–108.
2. Silverman KJ, Hutchins GM, Bulkley BH. Cardiac sarcoid: a clinicopathologic study of 84 unselected patients with systemic sarcoidosis. *Circulation* 1978;**58**:1204–11.
3. Wicks EC, Menezes LJ, Elliott PM. Improving the diagnostic accuracy for detecting cardiac sarcoidosis. *Expert Rev Cardiovasc Ther* 2015;**13**:223–36.
4. Soejima K, Yada H. The work-up and management of patients with apparent or subclinical cardiac sarcoidosis: with emphasis on the associated heart rhythm abnormalities. *J Cardiovasc Electrophysiol* 2009;**20**:578–83.
5. Perry A, Vuitch F. Causes of death in patients with sarcoidosis. A morphologic study of 38 autopsies with clinicopathologic correlations. *Arch Pathol Lab Med* 1995;**119**:167–72.
6. Uemura A, Morimoto S, Hiramitsu S, Kato Y, Ito T, Hishida H. Histologic diagnostic rate of cardiac sarcoidosis: evaluation of endomyocardial biopsies. *Am Heart J* 1999;**138**:299–302.
7. Diagnostic standard and guidelines for sarcoidosis. *Jpn J Sarcoidosis Granulomatous Disord* 2007;**27**:89–102.
8. Greulich S, Deluigi CC, Gloekler S, Wahl A, Zurn C, Kramer U *et al.* CMR imaging predicts death and other adverse events in suspected cardiac sarcoidosis. *JACC Cardiovasc Imaging* 2013;**6**:501–11.
9. Hamzeh NY, Wamboldt FS, Weinberger HD. Management of cardiac sarcoidosis in the United States: a Delphi study. *Chest* 2012;**141**:154–62.
10. Patel MR, Cawley PJ, Heitner JF, Klem I, Parker MA, Jaroudi WA *et al.* Detection of myocardial damage in patients with sarcoidosis. *Circulation* 2009;**120**:1969–77.
11. Ohira H, Tsujino I, Yoshinaga K. 18-F-Fluoro-2-deoxyglucose positron emission tomography in cardiac sarcoidosis. *Eur J Nucl Med Mol Imaging* 2011;**38**:1773–83.
12. Ohira H, Birnie DH, Pena E, Bernick J, Mc Ardle B, Leung E *et al.* Comparison of 18F-fluorodeoxyglucose positron emission tomography (FDG-PET) and cardiac magnetic resonance (CMR) in corticosteroid-naive patients with conduction system disease due to cardiac sarcoidosis. *Eur J Nucl Med Mol Imaging* 2016;**43**:259–69.
13. Langah R, Spicer K, Gebregziabher M, Gordon L. Effectiveness of prolonged fasting 18F-FDG PET-CT in the detection of cardiac sarcoidosis. *J Nucl Cardiol* 2009;**16**:801–10.
14. Soussan M, Brillet PY, Nunes H, Pop G, Ouvrier MJ, Naggara N *et al.* Clinical value of a high-fat and low-carbohydrate diet before FDG-PET/CT for evaluation of patients with suspected cardiac sarcoidosis. *J Nucl Cardiol* 2013;**20**:120–7.
15. Kramer CM, Barkhausen J, Flamm SD, Kim RJ, Nagel E. Society for Standardized cardiovascular magnetic resonance (CMR) protocols 2013 update. *J Cardiovasc Magn Reson* 2013;**15**:91.
16. Dickson JC, O'Meara C, Barnes A. A comparison of CT- and MR-based attenuation correction in neurological PET. *Eur J Nucl Med Mol Imaging* 2014;**41**:1176–89.
17. Ishimaru S, Tsujino I, Takei T, Tsukamoto E, Sakaue S, Kamigaki M *et al.* Focal uptake on 18F-fluoro-2-deoxyglucose positron emission tomography images indicates cardiac involvement of sarcoidosis. *Eur Heart J* 2005;**26**:1538–43.
18. Okumura W, Iwasaki T, Toyama T, Iso T, Arai M, Oriuchi N *et al.* Usefulness of fasting 18F-FDG PET in identification of cardiac sarcoidosis. *J Nucl Med* 2004;**45**:1989–98.
19. Keijsers RG, Verzijlbergen EJ, van den Bosch JM, Zanen P, van de Garde EM, Oyen WJ *et al.* 18F-FDG PET as a predictor of pulmonary function in sarcoidosis. *Sarcoidosis Vasc Diffuse Lung Dis* 2011;**28**:123–9.
20. Youssef G, Leung E, Mylonas I, Nery P, Williams K, Wisenberg G *et al.* The use of 18F-FDG PET in the diagnosis of cardiac sarcoidosis: a systematic review and metaanalysis including the Ontario experience. *J Nucl Med* 2012;**53**:241–8.
21. Schoenfeld D. Partial residuals for the proportional hazards regression model. *Biometrika* 1982;**69**:239–41.
22. Ambler G, Seaman S, Omar RZ. An evaluation of penalised survival methods for developing prognostic models with rare events. *Stat Med* 2012;**31**:1150–61.
23. Smedema JP, Snoep G, van Kroonenburgh MP, van Geuns RJ, Dassen WR, Gorgels AP *et al.* Evaluation of the accuracy of gadolinium-enhanced cardiovascular magnetic resonance in the diagnosis of cardiac sarcoidosis. *J Am Coll Cardiol* 2005;**45**:1683–90.
24. Coleman GC, Shaw PW, Balfour PC Jr, Gonzalez JA, Kramer CM, Patel AR *et al.* Prognostic value of myocardial scarring on CMR in patients with cardiac sarcoidosis. *JACC Cardiovasc Imaging* 2017;**10**:411–20.
25. Hulten E, Agarwal V, Cahill M, Cole G, Vita T, Parrish S *et al.* Presence of late gadolinium enhancement by cardiac magnetic resonance among patients with suspected cardiac sarcoidosis is associated with adverse cardiovascular prognosis: a systematic review and meta-analysis. *Circ Cardiovasc Imaging* 2016;**9**:e005001.
26. Newsholme P, Newsholme EA. Rates of utilization of glucose, glutamine and oleate and formation of end-products by mouse peritoneal macrophages in culture. *Biochem J* 1989;**261**:211–8.
27. Yamagishi H, Shirai N, Takagi M, Yoshiyama M, Akioka K, Takeuchi K *et al.* Identification of cardiac sarcoidosis with (13)N-NH(3)/(18)F-FDG PET. *J Nucl Med* 2003;**44**:1030–6.
28. Nishiyama Y, Yamamoto Y, Fukunaga K, Takinami H, Iwado Y, Satoh K *et al.* Comparative evaluation of 18F-FDG PET and 67Ga scintigraphy in patients with sarcoidosis. *J Nucl Med* 2006;**47**:1571–6.
29. Ishimaru S, Tsujino I, Sakaue S, Oyama N, Takei T, Tsukamoto E *et al.* Combination of 18F-fluoro-2-deoxyglucose positron emission tomography and magnetic resonance imaging in assessing cardiac sarcoidosis. *Sarcoidosis Vasc Diffuse Lung Dis* 2005;**22**:234–5.
30. Ohira H, Tsujino I, Ishimaru S, Oyama N, Takei T, Tsukamoto E *et al.* Myocardial imaging with 18F-fluoro-2-deoxyglucose positron emission tomography and magnetic resonance imaging in sarcoidosis. *Eur J Nucl Med Mol Imaging* 2008;**35**:933–41.
31. Nekolla SG, Rischpler C, Batrice A, Schwaiger M. Cardiac PET/MRI. *Curr Cardiovasc Imaging Rep* 2013;**6**:158–68.
32. Rischpler C, Nekolla SG, Dregely I, Schwaiger M. Hybrid PET/MR imaging of the heart: potential, initial experiences, and future prospects. *J Nucl Med* 2013;**54**:402–15.
33. Nensa F, Poeppel TD, Beiderwellen K, Schelhorn J, Mahabadi AA, Erbel R *et al.* Hybrid PET/MR imaging of the heart: feasibility and initial results. *Radiology* 2013;**268**:366–73.
34. Nensa F, Kloth J, Tezgah E, Poeppel TD, Heusch P, Goebel J *et al.* Feasibility of FDG-PET in myocarditis: comparison to CMR using integrated PET/MRI. *J Nucl Cardiol* 2016; doi:10.1007/s12350-016-0616-y.
35. Tadamura E, Yamamuro M, Kubo S, Kanao S, Hosokawa R, Kimura T *et al.* Images in cardiovascular medicine. Multimodality imaging of cardiac sarcoidosis before and after steroid therapy. *Circulation* 2006;**113**:e771–3.
36. Schneider S, Batrice A, Rischpler C, Eiber M, Ibrahim T, Nekolla SG. Utility of multimodal cardiac imaging with PET/MRI in cardiac sarcoidosis: implications for diagnosis, monitoring and treatment. *Eur Heart J* 2014;**35**:312.
37. Nekolla SG, Martinez-Moeller A, Saraste A. PET and MRI in cardiac imaging: from validation studies to integrated applications. *Eur J Nucl Med Mol Imaging* 2009;**36**:S121–30.
38. Birnie DH, Sauer WH, Judson MA. Consensus statement on the diagnosis and management of arrhythmias associated with cardiac sarcoidosis. *Heart* 2016;**102**:411–4.
39. Boellaard R. Need for standardization of 18F-FDG PET/CT for treatment response assessments. *J Nucl Med* 2011;**52**:93–100.
40. Doughan AR, Williams BR. Cardiac sarcoidosis. *Heart* 2006;**92**:282–8.
41. Reiter T, Werner RA, Bauer WR, Lapa C. Detection of cardiac sarcoidosis by macrophage-directed somatostatin receptor 2-based positron emission tomography/computed tomography. *Eur Heart J* 2015;**36**:2404.
42. Vignaux O, Dhote R, Duboc D, Blanche P, Dusser D, Weber S *et al.* Clinical significance of myocardial magnetic resonance abnormalities in patients with sarcoidosis: a 1-year follow-up study. *Chest* 2002;**122**:1895–901.
43. Crouser ED, Ono C, Tran T, He X, Raman SV. Improved detection of cardiac sarcoidosis using magnetic resonance with myocardial T2 mapping. *Am J Respir Crit Care Med* 2014;**189**:109–12.